4242–4256 *Nucleic Acids Research, 2008, Vol. 36, No. 13* *Published online 25 June 2008*
doi:10.1093/nar/gkn385

Mechanism and substrate specificity of telomeric protein POT1 stimulation of the Werner syndrome helicase

Gregory Sowd[1], Ming Lei[2] and Patricia L. Opresko[1,*]

[1]Department of Environmental and Occupational Health, University of Pittsburgh Graduate School of Public Health, Pittsburgh, PA 15219 and [2]Department of Biological Chemistry, University of Michigan Medical School, Ann Arbor, MI 48109-0606, USA

Received April 28, 2008; Revised May 15, 2008; Accepted May 31, 2008

ABSTRACT

Loss of the RecQ helicase WRN protein causes the cancer-prone progeroid disorder Werner syndrome (WS). WS cells exhibit defects in DNA replication and telomere preservation. The telomeric single-stranded binding protein POT1 stimulates WRN helicase to unwind longer telomeric duplexes that are otherwise poorly unwound. We reasoned that stimulation might occur by POT1 recruiting and retaining WRN on telomeric substrates during unwinding and/or by POT1 loading on partially unwound ssDNA strands to prevent strand re-annealing. To test these possibilities, we used substrates with POT1-binding sequences in the single-stranded tail, duplex or both. POT1 binding to ssDNA tails did not alter WRN activity on nontelomeric duplexes or recruit WRN to telomeric ssDNA. However, POT1 bound tails inhibited WRN activity on telomeric duplexes with a single 3′-ssDNA tail, which mimic telomeric ends in the open conformation. In contrast, POT1 bound tails stimulated WRN unwinding of forked telomeric duplexes. This indicates that POT1 interaction with the ssDNA/dsDNA junction regulates WRN activity. Furthermore, POT1 did not enhance retention of WRN on telomeric forks during unwinding. Collectively, these data suggest POT1 promotes the apparent processivity of WRN helicase by maintaining partially unwound strands in a melted state, rather than preventing WRN dissociation from the substrate.

INTRODUCTION

Werner syndrome (WS) is a human segmental progeroid syndrome in which patients prematurely develop numerous aging-related diseases including cataracts, osteoporosis, atherosclerosis and cancer (1). This autosomal recessive disorder is caused by loss of the RecQ DNA helicase WRN (2). *Escherichia coli* and budding yeast have a single RecQ DNA helicase, whereas humans have five and mutations in three cause distinct cancer predisposition disorders (3). Mutations in BLM and RecQL4 result in Bloom syndrome (BS) and Rothmund–Thomson syndrome (RTS), respectively (3). WRN is unique among mammalian RecQ helicases in that the protein also has 3′ to 5′ exonuclease activity (4). RecQ helicases in general, although there may be exceptions, function during DNA replication to prevent replication fork demise and to restore stalled or broken replication forks, partly through homologous recombination (HR) pathways (5). Consistent with this, WRN protein is implicated in several pathways for recombinational repair of stalled replication forks and DNA double strand breaks (3,6).

Dysfunctional telomeres contribute to the WS pathology and cellular defects. Telomeres protect chromosome ends, and telomere dysfunction triggers cellular senescence, apoptosis or genomic instability and chromosome fusions (7). Knockout of *Wrn* in mice yields no obvious phenotype. However, *Wrn* loss in a setting of shortened telomeres achieved by breeding mice also null for telomerase results in nearly the full spectrum of WS phenotypes (8,9). Furthermore, the forced expression of active telomerase can partially suppress many of the primary defects in WS fibroblasts including premature senescence (10), sister telomere loss (11) and the accumulation of chromosomal aberrations (12). These findings indicate that critically short telomeres contribute to genomic instability and senescence in WS, and that telomerase may compensate for WRN roles at telomeres.

Human telomeres consists of 2–10 kb of duplex TTAGGG repeats ending in a 3′-ssDNA tail and are bound by protein complexes termed shelterin or telosome (7). Telomeres exist in an open accessible form, and a closed inaccessible form which is proposed to involve invasion of the 3′-tail into the telomeric duplex to form

*To whom correspondence should be addressed. Tel: +1 412 521 3034; Fax: +1 412 624 9361; Email: plo4@pitt.edu

the lasso-like t-loop/D-loop structures observed by electron microscopy (13). The shelterin proteins telomere repeat binding factors 1 and 2 (TRF1 and TRF2) bind duplex TTAGGG repeats (14,15), and protection of telomeres 1 (POT1) binds the sequence TTAGGGTTAG in the single-stranded regions (16). TRF2 recruits WRN to telomeric substrates (17,18), and POT1 stimulates WRN to unwind longer telomeric duplexes (19).

Evidence indicates that WRN and POT1 may cooperate in common pathways at telomeric ends. WRN localizes to telomeres in S-phase telomerase deficient cells and suppresses loss of telomeres that are replicated from the G-rich lagging strand (11,20). Thus, WRN is proposed to dissociate potential replication fork blocks including G-quadruplexes that can form in TTAGGG repeats (21) and recombination-type D-loops that stabilize the telomeric t-loops (13). Quadruplex DNA, Holliday junctions and D-loops are preferred substrates for the WRN helicase *in vitro* (20,22,23). WRN suppresses sister chromatid exchanges at telomeres (24) consistent with roles in regulating telomeric recombination. Telomere defects in mouse cells null for Pot1a also indicate roles for POT1 in lagging strand telomere replication and in regulating telomeric recombination (25,26).

WRN helicase readily unwinds 20–30 bp duplexes, but poorly unwinds longer duplexes suggesting that the enzyme is weakly processive (27). POT1 stimulates WRN helicase to unwind longer telomeric duplexes that are otherwise not completely unwound, but does not directly alter the WRN exonuclease catalytic activity (19). The only other protein reported to date that enables WRN unwinding of longer duplexes is replication protein A (RPA), which also interacts with WRN (27). Unlike RPA which has no sequence specificity, POT1 could not pre-load on the ssDNA tails of previously tested forks in which the telomeric repeats were confined to the duplex region (19). Thus, to determine the substrate specificity and mechanism of POT1 stimulation of WRN helicase we examined a panel of substrates with POT1 binding sites in the ssDNA tails, duplex or both regions that mimic replication forks and open telomeric ends. We reasoned that helicase stimulation occurs by POT1 recruitment and retention of WRN on the telomeric substrate to increase unwinding processivity, and/or by POT1 binding to partially unwound strands to prevent their re-annealing upon WRN dissociation. We observed that POT1 preloading differentially regulated WRN activity on a 3′-tailed telomeric duplex compared to a telomeric fork, and that POT1 did not enhance retention of WRN on the substrate during unwinding. Collectively, our data support POT1 maintenance of partially unwound strands as the primary mode of WRN helicase stimulation.

MATERIALS AND METHODS

Proteins

Recombinant histidine-tagged WRN protein and the exonuclease-dead E84A mutant (X-WRN) were purified using a baculovirus/insect cell expression system and an AKTA Explorer FLPC (GE Life Sciences, Piscataway, NJ, USA) as previously (20) with some modification. Briefly, Sf9 insect cells expressing recombinant WRN or X-WRN were lyzed in Buffer A (20 mM Na_2HPO_4, 300 mM NaCl, 10% glycerol, 0.5% Igepal CA-630, 10 mM imidazole, 5 mM β-mercaptoethanol) with a protease inhibitor cocktail (Roche Molecular Biochemicals, Indianapolis, IN, USA) for 30 min at 4°C. Subsequent buffers contained protease inhibitors, 1 mM AEBSF and 5 mM β-mercaptoethanol. Following sonication, the lysate was centrifuged and the supernatant was precipitated in 40% saturation of ammonium sulfate then centrifuged at 12 000 r.p.m. for 30 min. The resulting pellet was resuspended in Buffer B (20 mM Na_2HPO_4, 300 mM NaCl, 10% glycerol, 0.05% Igepal CA-630) with 10 mM imidazole and loaded onto a HisTrap FF column (GE Life Sciences), followed by washing and elution with 100 and 250 mM imidazole, respectively, in buffer B. WRN fractions were loaded onto a HiLoad 16/60 Superdex 200 GL column (GE Life Sciences) equilibrated in buffer C (150 mM Tris pH 8.0, 0.05% Igepal CA-630, 10% glycerol) with 50 mM NaCl. Collected WRN fractions were then loaded onto a Resource Q column (GE Life Sciences) washed with increasing NaCl concentrations and eluted with 275 mM NaCl in buffer C. Recombinant human POT1 protein was purified using a baculovirus/insect cell expression system as described previously except two GSTrap columns (GE Life Science) were used (16). Protein concentration was determined by Bradford Assay (BioRad, Hercules, CA, USA) and purity was determined by SDS–PAGE and Coomassie staining. Recombinant RPA was kindly provided by Dr Walter Chazin (Vanderbilt University, TN, USA). Purified *E. coli* RecQ was generously provided by Dr James Keck (University of Wisconsin, WI, USA).

DNA substrates

All oligonucleotides for substrate preparations were from Integrated DNA Technologies, Coralville, IA, USA and were PAGE purified by the manufacturer. Oligonucleotides that were 5′-end labeled with [γ-^{32}P] ATP (3000 Ci/mmol) using T4 polynucleotide kinase (New England BioLabs, Ipswich, MA, USA) are indicated by an '*' in Table 1. Forked duplexes Tel 5′ss-34, Tel 5′ss-22 and Tel 3′ss-22 were constructed by annealing 9 pmol of the 5′-end-labeled oligonucleotide with 20 pmol of the complementary strand (marked 'compl' in Table 1) in 50 µl reactions with 50 mM LiCl at 95°C for 5 min, followed by cooling to room temperature. Construction and sequences of the Tel ds-34, Mix ds-34 and Mix ds-22 forks were as previously described (17,28). The fluorescently labeled TAMRA Tel ds-34 and Cy5 Mix ds-22 forks contained either a TAMRA or Cy5 fluorescent molecule covalently attached to the 5′-nucleotide. The Cy5 Mix ds-22 fork also contained a phosphorothioate linkage at the 3′-blunt end to inhibit exonuclease activity.

The 3′-tailed duplex and fork duplex substrates with telomeric sequence in the duplex region and variable sequences in the 3′-tail (Figures 3 and 5), were formed by annealing a long oligonucleotide into a hairpin to ensure proper alignment of the telomeric repeats (Table 1).

Table 1. Oligonucleotides used in substrate preparations

Name	Sequence (5′ to 3′)
Tel 5′ss-34	*TTAGGGTTAGGGTTAGGGTTAGGGGGTGATGGTGTATTGAGTGGGATGCATGCACTAC
Tel 5′-34 compl	GTAGTGCATGCATCCCACTCAATACACCATCACCTTTTTTTTTTTTTTT
Tel 5′-22	*TTAGGGTTAGGGTTAGGGTTAGGGCAGTGTGGTGTACATGCACTAC
Tel 5′ss-22 compl	GTAGTGCATGTACACCACACTGTTTTTTTTTTT
Tel 3′ss-22	*TTTTTTTTTTTTTTGAGTGTGGTGTACATGCACTAC
Tel 3′ss-22 compl	GTAGTGCATGTACACCACACTCTTAGGGTTAGGGTTAGGG
BioTel	Biotin-TTAGGGTTAGGGTTAGGGTTAGGGTTAGGGTTAG
36-bp substrates with telomeric repeats in the duplex and variable 3′tail sequences	
Mix Tailed duplex	*CTAACCCTAACCCTAACCCTAAGTTCATCCAGTGAT~~ATCCGTTTTCGGAT~~ATCACTGGATGAACTTAGGG TTAGGGTTAGGGTTAGCTGTTTGCATCGATCTGC
Tel Tailed duplex	*CTAACCCTAACCCTAACCCTAAGTTCATCCAGTGAT~~ATCCGTTTTCGGAT~~ATCACTGGATGAACTTAGGG TTAGGGTTAGGGTTAGGGTTAGGGTTAGGG
Mix Tail fork	*TTTCTCGTTTCTAACCCTAACCCTAACCCTAAGTTCATCCAGTGAT~~ATCCGTTTTCGGAT~~ATCACTGGATG AACTTAGGGTTAGGGTTAGGGTTAGCTGTTTGCATCGATCTGC
Tel Tail fork	*TTTCTCGTTTCTAACCCTAACCCTAACCCTAAGTTCATCCAGTGAT~~ATCCGTTTTCGGAT~~ATCACTGGATG AACTTAGGGTTAGGGTTAGGGTTAGGGTTAGGG
Tel-A Tail fork	*TTTCTCGTTTCTAACCCTAACCCTAACCCTAAGTTCATCCAGTGAT~~ATCCGTTTTCGGAT~~ATCACTGGATG AACTTAGGGTTAGGGTTAGGGTTAGGGTTACGGTTAGGGTTAGGG
Tel-B Tail fork	*TTTCTCGTTTCTAACCCTAACCCTAACCCTAAGTTCATCCAGTGAT~~ATCCGTTTTCGGAT~~ATCACTGGATG AACTTAGGGTTAGGGTTAGGGTTAGGGTTAGGGCTTAGGG
Tel-G Tail fork	*TTTCTCGTTTCTAACCCTAACCCTAACCCTAAGTTCATCCAGTGAT~~ATCCGTTTTCGGAT~~ATCACTGGATG AACTTAGGGTTAGGGTTAGGGTTAGGGTTAGGGTTAG

*Donates 5′-end radio-label.
Underlining indicates nucleotides in the ssDNA tail regions.
Bolding and strike through indicates nucleotides that were lost upon digestion of the hairpins with EcoRV.

The 5′-end-labeled oligonucleotides were annealed at 95°C for 5 min, cooled stepwise (1.2°C/min) to 60°C, incubated for 1 h, and then cooled stepwise (1.2°C/min) to 25°C. The hairpins were restricted with EcoRV (New England BioLabs) to generate a blunt end, and substrates were purified by PAGE and Qiaex II Gel Extraction Kit (Qiagen, Valencia, CA, USA). Purification yields were determined by phosphorimager analysis.

Helicase and exonuclease reactions

Reactions were performed in standard reaction buffer (28) unless otherwise indicated. DNA substrate and protein concentrations were as indicated in the figure legends. The reactions were initiated by adding WRN protein and were incubated at 37°C for 15 min. For analysis of radio-labeled molecules on 12% native polyacrylamide gels, the reactions (20 μl) were stopped with 10 μl of 3× stop dye supplemented with 10 μg/ml proteinase K and 10× molar excess of unlabeled competitor oligonucleotide (28) and deproteinized for 30 min at 37°C. The reactions in Figures 3 and 5 for substrates generated from hairpin forming olignucleotides were loaded directly on 12% native polyacrylamide gels containing 0.1% SDS following termination to avoid bi-molecular quadruplex formation and lacked competitor oligonucleotides in the stop dye. Products were visualized using a Typhoon phosphorimager and quantified using ImageQuant software (GE Life Sciences).

For the fluorescent substrate retention assays (Figure 7), aliquots were removed at the times indicated in the figure legend and terminated by adding 10 μl of 3× stop solution (15 mM EDTA, 30% glycerol, 10 μg/ml Proteinase K) and unlabeled competitor oligonucleotides. Reactions were deproteinized for 15 min at 37°C, separated on a 12% native polyacrylamide gel, and analyzed by fluoroimagery using a Typhoon Imager and ImageQuant software (GE Life Sciences). The reactions in Figure 7A–D containing equal molar TAMRA Tel ds-34 and Cy5 Mix ds-22 forks with or without POT1 were initiated by WRN addition. The reactions in Figure 7E containing POT1 and TAMRA Tel ds-34 fork were initiated by adding X-WRN. After 5 min of reaction, a 10× molar excess of cold competitor nontelomeric Mix ds-34 fork was added, where indicated, to trap any dissociated WRN protein (Figure 7E).

For quantitation of strand displacement, the percent of unreacted substrate and the percent of each major product band in the native gels were calculated as a fraction of the total radioactivity or fluorescence in the reaction lane (20). The product bands were summed to calculate the percent of total displacement (Figures 2, 3, 5–7). The percent displacement of strands with intact telomeric sequence were calculated by summing strands ≥39 nt (Figure 2) or ≥33 nt (Figure 5). In Figure 5C, the percent of displaced products with intact telomeric sequence for reactions with WRN and POT1 were normalized by dividing by the product values for reactions containing only WRN. All values were corrected for background in the no enzyme control and heat denatured substrate lanes.

Telomeric ssDNA-binding assay

The reactions (20 μl) were performed in standard reaction buffer (40 mM Tris pH 8.0, 4 mM $MgCl_2$, 5 mM DTT, 100 ng/μl BSA, 0.1% Tween 20 and 2 mM ATP) with

50 mM LiCl to prevent quadruplex formation. DNA substrate and protein concentrations were as indicated in the figure legend. The biotinylated single-stranded telomeric oligonucleotide BioTel (Table 1) was preincubated with POT1 for 5 min at room temperature. Reactions were initiated by adding WRN, incubated at 37°C for 15 min and then incubated with 100 μg of prewashed Streptavidin magnetic particles (Roche Biochemicals) with continuous mixing for 10 min at 25°C. The beads were harvested with a magnet, the supernatant was recovered and the pellet was washed twice in standard buffer lacking ATP. Protein–DNA complexes were eluted at 95°C for 5 min in LDS loading buffer (Invitrogen, Calsbad, CA, USA) and 100 mM β-mercaptoethanol. The protein in the supernatant and pellet were analyzed by western blotting with mouse monoclonal anti-WRN [1 : 20 dilution, (29)] and rabbit polyclonal anti-POT1 (1 : 500 dilution, Imgenex).

RESULTS

Two possible mechanistic models for POT1 stimulation of WRN are shown in Figure 1, which schematically displays WRN activity on a telomeric duplex fork with and without POT1, according to previous observations (19). The substrate (Tel ds-34 fork) has 15-mer ssDNA poly-T tails at one end followed by a duplex of four TTAGGG repeats and 10-bp of unique sequence (28). The model also applies to observations made with a telomeric D-loop (19). Upon substrate binding, WRN helicase unwinds at the forked end and the exonuclease initiates digestion at the blunt end and progresses 3′ to 5′ (Figure 1B) (28). Blunt ended duplex DNA is normally not a WRN substrate, but WRN loading at forks or junctions activates digestion at blunt ends of numerous types of substrates (23,28,30,31). Once the DNA strand is unwound, further digestion is severely limited (Figure 1, depicted with an X), since WRN exonuclease activity is inefficient on relatively short ssDNA strands (limited to 1–4 nt), compared to duplex DNA and very long ssDNA strands (Figure S1, Supplementary data) (28,32–36). Thus, if WRN displaces the duplex in one binding cycle there is less opportunity for extensive strand digestion (Figure 1D). However, if WRN dissociates prior to complete strand displacement, the partially unwound strands (dotted lines in Figure 1) re-anneal so that upon rebinding the helicase must initiate

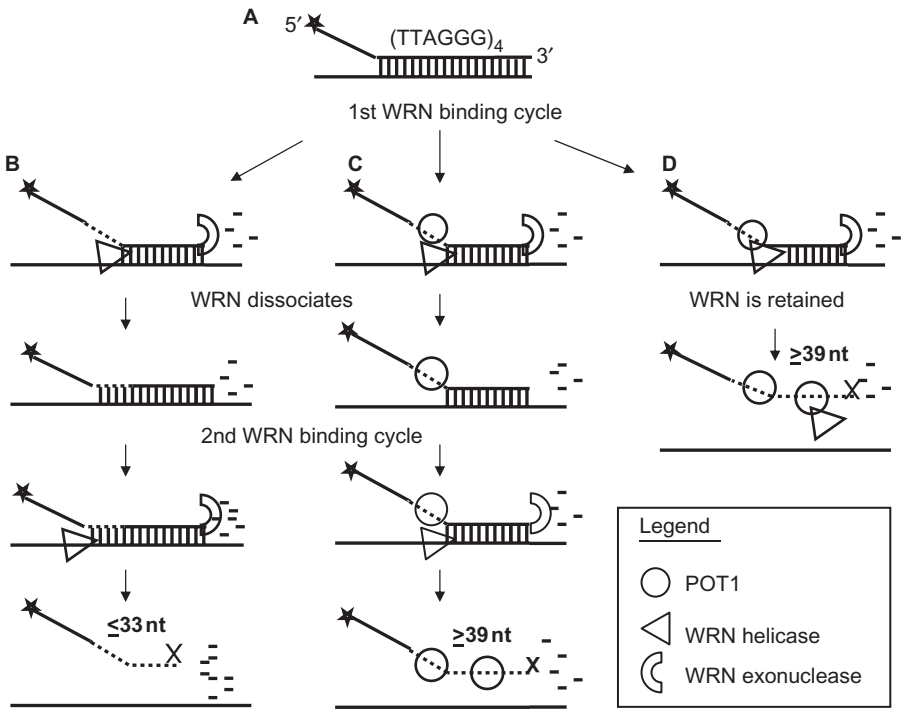

Figure 1. Models for POT1 mediated increase in WRN displacement of longer strands from a telomeric forked duplex. (**A**) The 34-bp telomeric fork contains four TTAGGG repeats in the duplex, which is shortened due to the action of the WRN helicase (triangle) unwinding at the forked end and WRN exonuclease (crescent) digesting at the blunt end (**B**). WRN domains are depicted as separate species for simplicity since the oligomeric form of active WRN is unknown. If WRN dissociates prior to duplex shorting to unstable lengths the partially unwound strands reanneal (dotted line; B). Upon WRN re-binding, the helicase must unwind again at the initial duplex start, whereas the exonuclease resumes digestion from the point of termination prior to WRN dissociation. This results in further strand digestion before it is completely displaced and becomes a poor substrate for the WRN exonuclease (indicated by an X; B). Multiple rounds of WRN binding/activity may occur for some molecules (two are shown), leading to a product distribution of multiple strand sizes (majority ≤33 nt, see Figure 2A). POT1 shifts the product distribution to favor displacement of longer strands (majority ≥39 nt, see Figure 2A). POT1 may bind the TTAGGG repeats of the top strand during unwinding and prevent strand re-annealing upon WRN dissociation (**C**). When WRN rebinds, unwinding can ensue at the point of termination prior to WRN dissociation, resulting in more rapid displacement of the remaining duplex and less digestion. Alternatively, POT1 may retain WRN on the telomeric fork during unwinding, so the fork is rapidly unwound in one WRN binding cycle and digestion is limited (**D**).

again, whereas the exonuclease resumes from the point of protein dissociation. This causes more extensive strand digestion and a product distribution of various lengths (Figures 1B and 2A, lane 2) (28). Thus, the extent of exonuclease digestion serves as a tool for monitoring helicase progression and apparent processivity. Increased helicase processivity correlates with longer displaced strands and less opportunity for digestion, since unwinding progresses more rapidly than digestion (28). Adding POT1 to the WRN reactions results in a dose-dependent loss of shorter

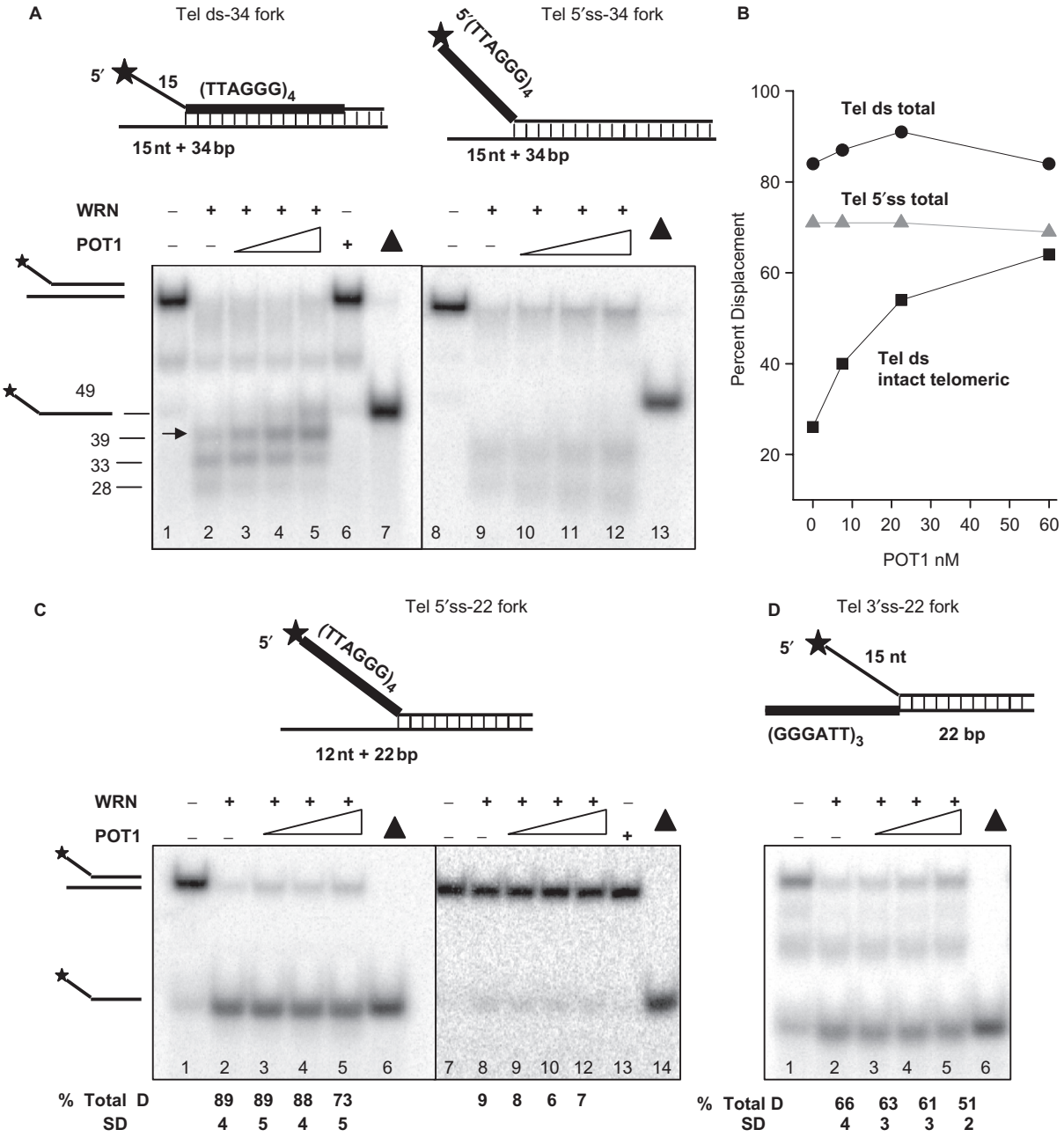

Figure 2. POT1 preloading on telomeric tails is insufficient to stimulate WRN helicase activity. (**A**) Reactions contained a 34-bp forked duplex (0.5 nM) with TTAGGG repeats (thick black line) in either the duplex (Tel ds-34 fork, lanes 1–7) or the 5′-ssDNA tail (Tel 5′ss-34 fork, lanes 8–13). The substrate was incubated with either 7.5 nM WRN alone (lanes 2 and 9) or with increasing POT1 (7.5, 22.5 and 60 nM) (lanes 3–5 or 10–12, respectively), for 15 min under standard reaction conditions. Arrow points to displaced 39-nt strands with intact telomeric sequence. Numbers represent product sizes for the Tel ds-34 fork. (**B**) The percent displacement of total products (Tel ds-34 fork, black circles; Tel 5′ss-34 fork, gray triangles), and the percent displacement of strands with intact telomeric sequence (≥39 nt) (Tel ds-34 fork, black squares) were plotted against POT1 concentration. (**C** and **D**) A 22-bp forked duplex (0.5 nM) with TTAGGG repeats (thick black line) in the 5′-ssDNA tail (C) or the 3′-ssDNA tail (D) was incubated with WRN alone or with increasing POT1 for 15 min under standard reaction conditions. In (C), WRN amounts were 0.38 nM (lanes 2–5) and 0.12 nM (lanes 8–12), and POT1 amounts were 0.38, 1.1 or 3.0 nM (lanes 3–5) and 0.12, 0.38 and 1 nM (lanes 9–12), respectively. In (D), WRN was 0.25 nM (lanes 2–5) and POT1 amounts were 0.25, 0.75 or 2 nM (lanes 3–5), respectively. All reactions were run on a 12% native gel. Filled triangle, heat denatured substrate. The percent total displacement (D) was calculated as described in Materials and methods section. Values for (C) (lanes 1–6) and (D) represent the mean and SD from three to four independent experiments.

products in favor of the longer products (Figures 1C, D and 2A, lanes 1–7). POT1 may increase the apparent processivity of WRN helicase by acting as a clamp to retain WRN so complete unwinding is achieved in one binding cycle (Figure 1D). Alternatively, POT1 binding to partially unwound strands may prevent their re-annealing upon helicase dissociation, so WRN can resume unwinding from the point of protein dissociation (Figure 1C). These possibilities are not mutually exclusive, and would shift the WRN product distribution toward displacement of longer strands.

POT1 preloading is insufficient to stimulate WRN helicase activity

We first tested whether POT1 recruitment of WRN to forked substrates was sufficient to stimulate the helicase activity. For this, the four TTAGGG repeats in the duplex region of the previously tested Tel ds-34 fork were moved to the 5′-ssDNA tail (5′Tel ss-34 fork), so POT1 could preload prior to WRN unwinding of the now nontelomeric duplex (Figure 2A, lanes 8–13). Preincubation of the 5′Tel ss-34 fork with increasing POT1 did not alter the product distribution generated by the combined action of the WRN helicase and exonuclease (Figure 2A lanes 8–13). This is in stark contrast to reactions with the fork containing telomeric repeats in the duplex (Tel ds-34 fork), used as a positive control, in which POT1 shifts the product distribution toward longer strands with intact telomeric repeats ($\geq$39-nt long) (Figure 2A, lanes 1–5, arrow; and Figure 2B, squares). POT1 also stimulates unwinding of the Tel ds-34 fork by an exonuclease-dead WRN mutant, but does not alter exonuclease digestion in the absence of helicase unwinding (19). Total strand displacement remained high for both fork substrates in the presence of POT1 (Figure 2B). Therefore, POT1 preloading did not alter the WRN helicase apparent processivity on a nontelomeric duplex.

To determine the effect of POT1 preloading on WRN helicase activity more directly, we tested forks with a shorter duplex (22 bp) that could be fully unwound by the WRN helicase. These substrates contained TTAGGG repeats on either the 5′- or 3′-ssDNA tails. As shown previously (28), WRN rapidly and completely displaces short 22-bp forks so that digestion by the exonuclease is minimal (Figure 2C and D, lane 2). Preincubation with increasing POT1 amounts did not significantly alter the percent of total strand displacement for either substrate (Figure 2C and D, lanes 1–6), even when lower WRN amounts were used (Figure 2C, lanes 7–14). This contrasts with TRF2 protein, which increases the percent of 22-bp forks unwound by WRN regardless of the duplex sequence (17). Collectively, these data indicate that POT1 preloading on ssDNA tails is not sufficient to stimulate WRN helicase either by increasing the apparent processivity (Figure 2A lanes 8–13) or the percent of total unwound substrates (Figure 2C and D). Therefore, POT1 recruitment of WRN to telomeric substrates is unlikely the primary mechanism of stimulation.

POT1 inhibits WRN activity on 3′ telomeric tailed substrates

The failure of POT1 to stimulate WRN helicase on the nontelomeric duplexes with telomeric tails in Figure 2, suggests that stimulation requires POT1-binding sequences in the duplex region. Therefore, we next tested substrates with telomeric sequence in both the duplex and ssDNA regions. While POT1 preloading is not sufficient to stimulate WRN helicase (Figure 2), we hypothesized that POT1 preloading might further increase stimulation of WRN unwinding of telomeric duplexes. Substrates that resemble telomeric ends in the open accessible form were prepared in which the telomeric duplex is followed by an exposed 3′-ssDNA tail with TTAGGG repeats (37). WRN helicase translocates along ssDNA with 3′ to 5′ polarity during duplex unwinding and can unwind duplexes with a 3′-ssDNA tail, but not a 5′-ssDNA tail (38). We constructed 36-bp duplexes with 14 bp of unique sequence followed by 22 bp of $(TTAGGG)_3TTAG$ sequence and an ssDNA 3′-tail with either $GG(TTAGGG)_3$ (Tel Tailed duplex) or a scrambled sequence (Mix Tail duplex) (see Materials and methods section). The shorter strand of the duplexes (Figure 3A, gray) contained the 5′-sequence (ATC-5′) most frequently found at telomeres *in vivo* (39) (Table 1). A band migrated above the substrate for the Tel Tail duplex (Figure 3A, lane 1, gray arrow), which disappeared after WRN addition (lanes 2–5), boiling (lane 6) or replacement with a nontelomeric tail (Figure 3B). Thus, this upper band likely represents bi-molecular G-quadruplex structures that formed between ssDNA tails of two independent molecules during the substrate purification.

Similar to the forks, WRN displaced shortened strands from the 3′-tailed duplexes due to the WRN exonuclease acting at the 3′-OH of the blunt end (Figure 3A and B, lane 2). Such a blunt end would not normally exist at the telomere in the context of a chromosome unless a break occurred. Rather, the exonuclease activity in these experiments serves as a biochemical tool for monitoring the helicase apparent processivity, since digestion proceeds much further in the absence of helicase activity (Figure S2, Supplementary data) similar to fork substrates (28). Surprisingly, preincubation of the Tel Tail duplex with increasing POT1 amounts led to a dose-dependent inhibition of WRN activity (Figure 3A, lanes 1–7, and Figure 3C). The percent of unreacted substrate increased nearly 6-fold from 11% to 62% at the highest POT1 amount (Figure 3C). In agreement with previous reports (32–34,40), we find relatively short 3′-ssDNA tails (18-nt long) are poor substrates for WRN exonuclease (Figure S1, Supplementary data) thus, the 3′-tails are present for WRN or POT1 loading in these experiments. Similar levels of WRN inhibition occurred when the telomeric 3′-tail ended in the optimal POT1-binding sequence (TAG-3′) (data not shown). WRN inhibition occurred even in the absence of helicase activity (Figure S2, Supplementary data) and was dependent on POT1 binding to the 3′-tail. POT1 preincubation with the Mix Tail duplex caused weak WRN inhibition only at the highest POT1 amount (Figure 3C). In contrast to POT1,

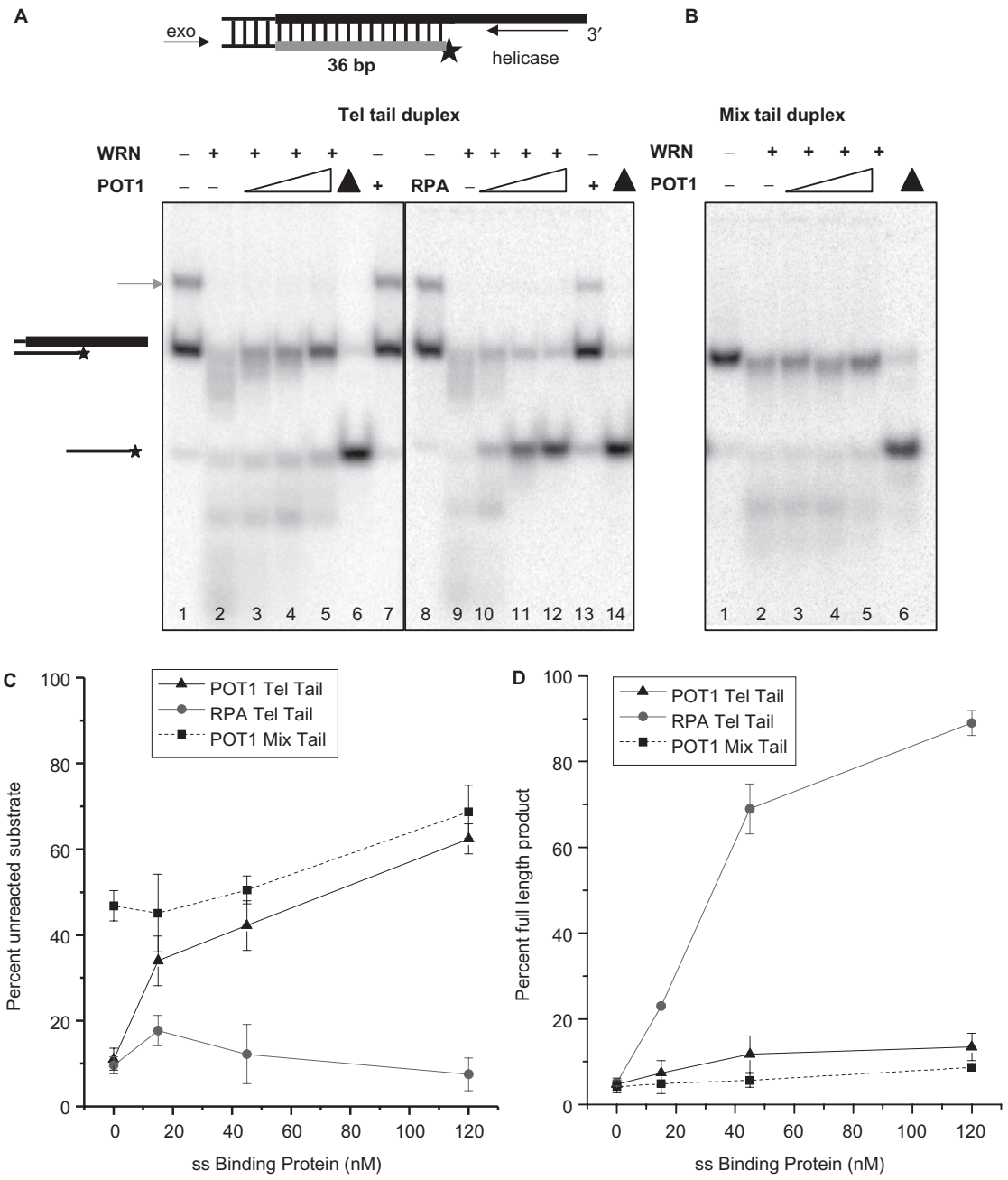

Figure 3. POT1 inhibits WRN activity on a model telomeric 3′-tailed duplex. Reactions contained a 36-bp tailed duplex (0.5 nM) with the $(TTAGGG)_3TTAG$ sequence in the duplex region followed by a 3′-ssDNA tail with either the sequence $GG(TTAGGG)_3$ (**A**) or 18 nt of scrambled sequence (**B**). The substrate was incubated with 15 nM WRN protein alone (lanes 2 and 9) or with increasing POT1 (15, 45 or 120 nM) (lanes 3–5, A and B) or RPA (15, 45 and 120 nM) (lanes 10–12, A) for 15 min under standard reaction conditions. Reaction products were separated on a 12% native gel. Filled triangle, heat denatured substrate. (**C**) The percent of unreacted substrate was calculated as a function of total radioactivity (see Materials and methods section) and plotted against POT1 or RPA concentration. (**D**) The percent of displaced full-length strands was calculated as a function of total radioactivity (see Materials and methods section) and plotted against POT1 or RPA concentration. POT1 and Tel Tail duplex, filled triangle and solid line; POT1 and Mix Tail duplex, filled square and dotted line; RPA and Tel Tail duplex, filled circle and gray line. Values represent the mean and error bars represent the SD of three independent experiments.

preincubation of the Tel Tail duplex with RPA caused a dramatic dose-dependent increase in WRN displacement of full-length strands, up to 19-fold (Figure 3A lanes 8–14, Figure 3D), and no inhibition (Figure 3C). These studies indicate that POT1 preloading on a 3′-tailed duplex causes WRN inhibition, whereas RPA increases the apparent WRN helicase processivity.

WRN can load on POT1 coated telomeric ssDNA

To determine whether POT1 preloading on the 3′ telomeric tails was inhibiting WRN loading, we performed binding assays under the identical reaction conditions as the helicase assays. Biotinylated $(TTAGGG)_5$ oligonucleotides unbound or precoated with POT1 protein

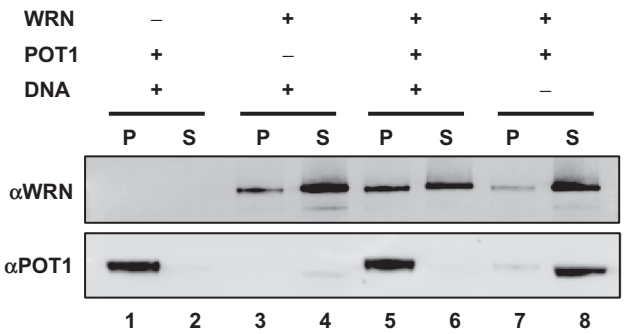

Figure 4. WRN binds to POT1 coated telomeric single-stranded oligonucleotides. The 5′ biotinylated telomeric oligonucleotides (BioTel, 250 nM) were preincubated alone or with POT1 (750 nM) at 4°C, followed by adding WRN (94 nM) where indicated for 15 min at 37°C. The oligonucleotides were captured with strepavidin beads and the bound proteins in the pellet (P) and unbound proteins in the supernatant (S) were analyzed by SDS–PAGE and probed for WRN and POT1 by Western blot. 25% of the supernatant and 25% of the pellet fractions were loaded.

were mixed with WRN, precipitated with streptavidin beads and then unbound protein in the supernatant and bound protein in the pellet were analyzed (Figure 4). The oligonucleotides contained three nonoverlapping POT1-binding sites. Therefore, a 3-fold molar excess of POT1 was added to ensure saturation of the POT1-binding sites, as confirmed by the presence of POT1 in the pellet and negligible amounts in the supernatant (Figure 4, lanes 1 and 2). In contrast, WRN addition to the oligonucleotides alone resulted in a higher fraction of WRN in the unbound supernatant, relative to the pellet, due to a lower affinity for ssDNA compared to POT1 (Figure 4, lanes 3 and 4). Adding WRN protein to POT1 coated oligonucleotides did not alter the amount of bound WRN protein recovered in the pellet (Figure 4, lane 5), compared to pellets from uncoated oligonucleotides (lane 3) (ratio is 0.96 ± 0.12, as averaged from five independent experiments). Furthermore, the ratio of WRN amount in the pellet versus supernatant was 0.71 ± 0.19 for naked DNA (Figure 4, lanes 3 and 4) and 0.79 ± 0.06 for POT1 coated DNA (Figure 4, lanes 5 and 6). Importantly, WRN protein did not cause any detectable dissociation of POT1 from the telomeric ssDNA (Figure 4, compare lanes 1 to 5 and 2 to 6). These data indicate that POT1 does not inhibit WRN from loading onto telomeric 3′-tails. Although we cannot rule out the possibility that WRN may bind the telomeric ssDNA partly through interaction with POT1, there was no obvious recruitment or enhancement of WRN binding by POT1.

POT1 binding to forked junctions stimulates the WRN helicase

POT1 preloading on the substrate does not prevent WRN binding to the DNA (Figure 4) or WRN unwinding of forked non-telomeric duplex (Figure 2C), but does inhibit WRN activity on a 3′-tailed telomeric duplex (Figure 3). Thus, POT1 binding might differ in the context of a 3′-tailed duplex compared to a forked duplex. POT1 ensures that the recessed 5′-end of telomeres terminates in the correct ATC-5′ sequence, suggesting that POT1 bound to the 3′-ssDNA tail of the telomere may also interact with, or occlude, the recessed 5′-end (39). Therefore, we next tested POT1 modulation of WRN activity on forks with telomeric sequence in both the duplex and the 3′-ssDNA tail. A 10 nt 5′-tail was added to the 36-bp 3′-tailed duplexes in Figure 3 to generate a variety of forks. The sequences of the 3′-tails are shown in Figure 5B. Similar to the Tel Tail duplex (Figure 3A), WRN displaced shortened strands from the Tel Tail fork due to exonuclease activity at the blunt end (Figure 5A, lane 2). In stark contrast to the Tel Tail duplex (Figure 3A), POT1 preloading on the Tel Tail fork did not inhibit WRN and shifted the WRN product distribution toward displacement of longer strands ($\geq$33 nt) in a dose-dependent manner (Figure 5). The ssDNA products $\geq$33 nt contain fully intact telomeric 5′CTAA$(CCCTAA)_3$ sequence (Table 1), indicating that POT1 prevented digestion into the telomere repeats past the 14 bp of unique sequence. POT1 promoted release of longer ssDNA strands by increasing the helicase apparent processivity, rather than by directly inhibiting the exonuclease for several reasons. First, POT1 did not alter the pattern of released products in the absence of helicase activity (Figure S3, Supplementary data). Second, in contrast the Tel ds-34 fork (Figure 2A), the strand that is extensively digested by WRN in the Tel Tail fork is not bound directly by POT1; the POT1 binding sequences are on the complementary strand. Therefore, POT1 could not simply block the progression of the exonuclease by binding the strand. In summary, adding a 5′-ssDNA tail to the Tel Tail duplex with a single 3′-tail (Figure 3A) abolished POT1 inhibition of WRN activity, and restores POT1 stimulation of WRN helicase.

To determine whether POT1 preloading on the 3′-tail enhances stimulation of WRN unwinding of the telomeric forks, we scrambled the sequence in the 3′-tail to prevent POT binding. POT1 addition resulted in a weak, but dose-dependent, increase in WRN displacement of strands with intact telomeric sequence ($\geq$33 nt) (Figure 5A, lanes 8–13). The higher level of stimulation with a telomeric 3′-tail (3.6-fold, Tel Tail fork), compared to a non-telomeric 3′-tail (1.5-fold, Mix Tail fork), indicates that POT1 preloading enhances stimulation of WRN helicase. Although both lack telomeric tails, the Mix Tail fork contains fewer complete TTAGGG repeats in the duplex than the Tel ds-34 fork (Figure 2A), and has the POT1 binding sites on the opposite strand. These differences might account for the weaker WRN stimulation on the Mix Tail fork, compared to the Tel ds-34 fork.

The 3′-tail of the Tel Tail fork duplex contains two mutually exclusive POT1 binding sites; one at the ssDNA/dsDNA junction and one closest to the 3′-end of the tail (Figure 5B). To determine which POT1 loading site is more critical for WRN stimulation, we mutated each site separately to abolish POT1 binding (Figure 5B). These mutations interrupted the guanine runs and caused a loss of the species that migrated above the substrate (Figure 5A, lanes 14–25, gray arrow), consistent with an inability to form bi-molecular G-quadruplexes. When the POT1-binding site nearest the

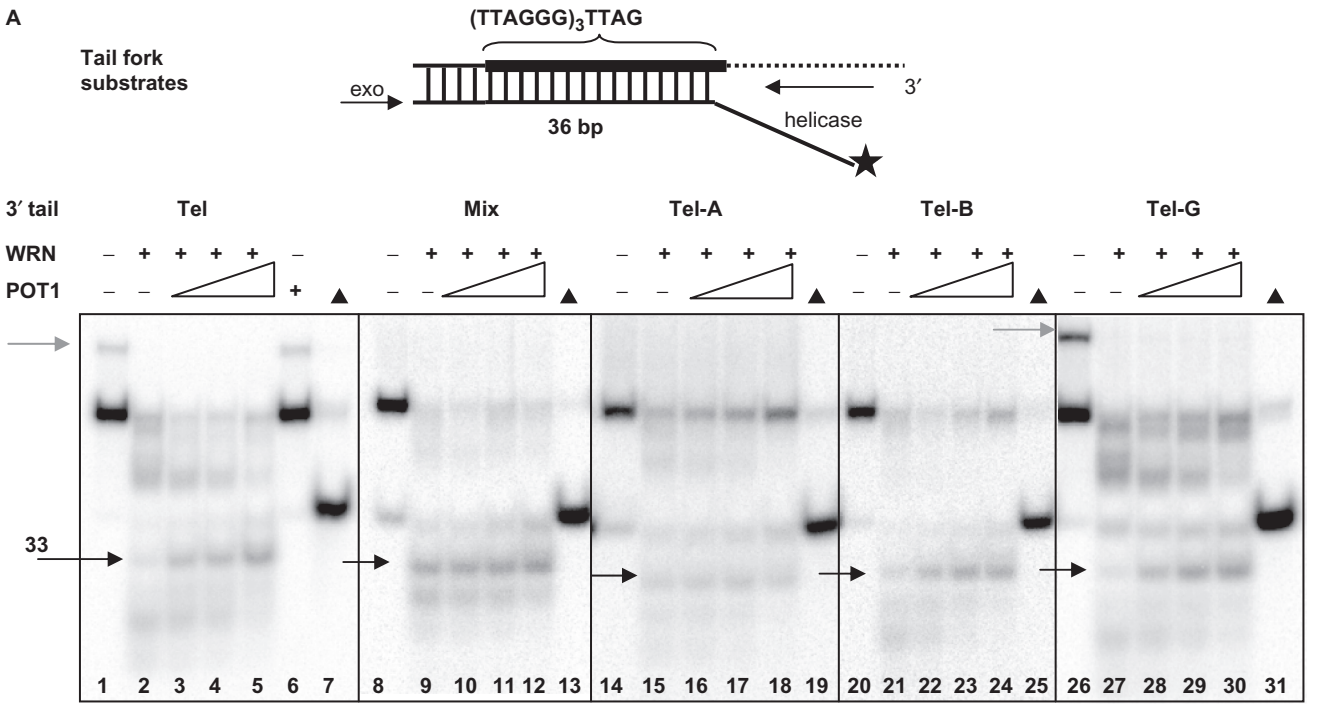

B

	3′ tail sequence: 5′ to 3′	Fold increase
Mix	CTGTTTGCATCGATCTGC	1.5
Tel	GGTTAGGGTTAGGGTTAGGG	3.7
Tel-A	GGTTACGGTTAGGGTTAGGG	1.8
Tel-B	GGTTAGGGTTAGGCTTAGGG	2.3
Tel-G	GGTTAGGGTTAGGGTTAG	2.6

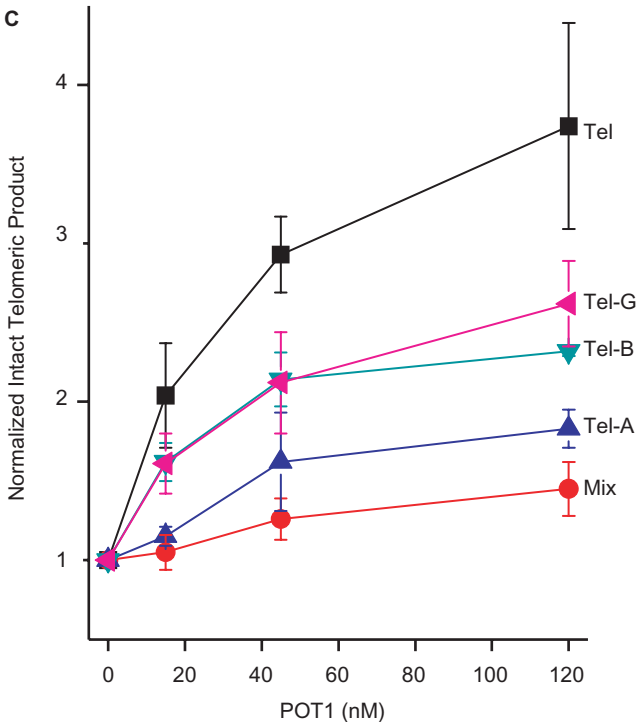

Figure 5. Addition of a 5′-ssDNA tail restores POT1 stimulation of WRN helicase on telomeric 3′-tailed duplexes. Reactions contained a 36-bp duplex (0.5 nM) with the $(TTAGGG)_3TTAG$ sequence in the duplex region followed by a 5′ 10-nt tail of unique sequence and a 3′-ssDNA tail with the sequences indicated in (**B**). Products were analyzed on 12% native gels. Filled triangle, heat denatured substrate. The arrow indicates the displaced strands (33 nt) with fully intact CTAA(CCCTAA)3 telomeric sequence in the 5′-end-labeled strand (star). (**A**) A 36-bp forked duplex with the 3′-tail containing the sequence Tel (lanes 1–7), Mix (lanes 8–13), Tel-A (lanes 14–19), Tel-B (lanes 20–25) or Tel-G (lanes 26–31) was incubated with WRN (15 nM) alone or with increasing POT1 (15, 45 or 120 nM) as indicated, for 15 min under standard reaction conditions. (B) Sequence of the 3′ telomeric tails. Boxes represent POT1-binding sites. The percent of displaced strands with fully intact telomeric sequence (≥33 nt) was calculated as a function of total radioactivity (see Materials and methods section). The fold increase in displaced intact telomeric strands at 120 nM POT1 relative to WRN alone is reported in (B), and the fold increase in displaced intact telomeric strands for each POT1 concentration relative to WRN is plotted against POT1 concentration in (**C**). The 3′-tail sequences Tel, filled square and black line; Mix, filled circle and red line; Tel-A, filled triangle and blue line; Tel-B, inverted filled triangle and green line; Tel-G, tilted filled triangle and pink line. Values represent the mean and error bars represent the SD from three independent experiments.

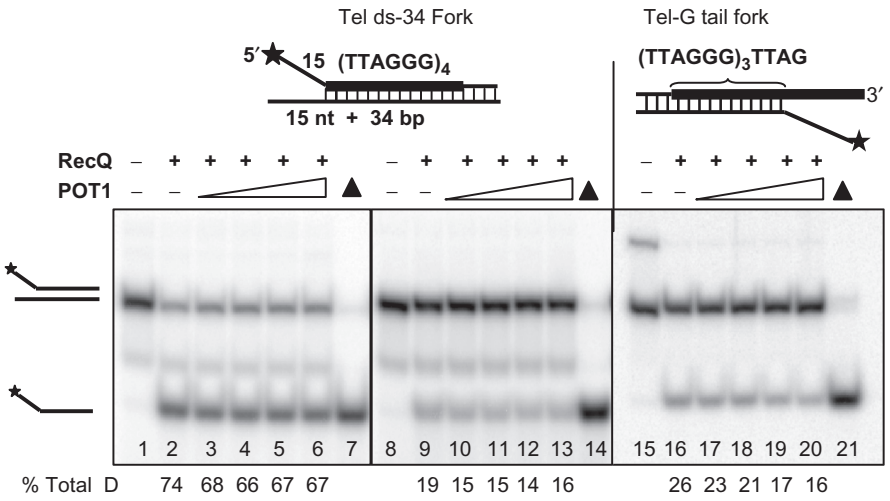

Figure 6. POT1 does not alter *E. coli* RecQ helicase unwinding of telomeric forks. Reactions contained a forked duplex with TTAGGG repeats (thick black line) in the duplex region alone (Tel ds-34 bp fork, 0.5 nM lanes 1–7, and 1 nM lanes 8–14) or in both the duplex and the 3′-ssDNA tail (Tel-G Tail fork, 0.5 nM lanes 15–21). The substrate was incubated with 0.12 nM RecQ protein alone (lanes 2, 9 and 16) or with increasing POT1 (0.12, 0.38, 1, or 2.5 nM, lanes 3–6 and 17–20) or (0.12, 0.38, 1 or 5 nM, lanes 10–13, respectively), for 15 min under standard reaction conditions. The percent total displacement was calculated as described in Materials and methods section.

junction was mutated (Tel-A Tail fork), the level and pattern of WRN stimulation was similar to that with the Mix Tail fork; up to a 1.8-fold increase (Figure 5A, lanes 14–19, and Figure 5B and C). Minor WRN inhibition occurred at the highest POT1 concentration, (Figure 5A, lane 14–19). In contrast to the Tel-A Tail fork, when the POT1-binding site nearest the 3′-end of the tail was mutated (Tel-B Tail fork), the level of WRN stimulation was similar to that observed on the Tel Tail fork (Figure 5A, lanes 20–25); up to a 2.3-fold increase (Figure 5B and C). These data indicate that the two POT1-binding sites have an additive effect on WRN stimulation, but that POT1 loading at the site closest to the junction contributes more to WRN stimulation.

Finally, we determined whether the terminal sequence of the telomeric 3′-tail would impact POT1 modulation of WRN activity. When the telomeric strand ends in the sequence 3′-TAG, POT1 tucks the end into a binding pocket (16) and inhibits telomerase activity *in vitro* (41). Changing the 3′-tail terminal sequence of the Tel Tail fork from -TAGGG (Tel) to -TAG (Tel-G) did not significantly alter POT1 stimulation of WRN helicase (Figure 5A, lanes 26–31, Figure 5B and C). Taken together, these data indicate that POT1 preloading near the forked junction enhances WRN helicase stimulation.

POT1 stimulation of WRN is species specific

POT1 stimulates WRN and BLM helicase activity, but not bacterial helicase UvrD (19), indicating that the functional interaction may be species specific. However, UvrD helicase is not a RecQ DNA helicase and may unwind DNA via a different mechanism. Therefore, we examined unwinding of telomeric forks by *E. coli* RecQ in the presence of POT1. RecQ exhibits robust unwinding of the Tel ds-34 fork and the Tel-G Tail fork and increased processivity compared to WRN (Figure 6, lanes 2 and 16). To improve detection of potential stimulation, RecQ unwinding of the Tel ds-34 fork was also lowered by increasing the substrate concentration (Figure 6, lanes 8–14). Adding up to a 40-fold molar excess of POT1 over RecQ did not significantly alter the amount of strand displacement (Figure 6). The two highest POT1 concentrations tested caused a weak inhibition of RecQ on the Tel-G Tail fork (~1.5-fold, Figure 6, lanes 19 and 20). The highest POT1 concentration (5 nM) was sufficient to stimulate unwinding of the Tel ds-34 fork by wild-type WRN, and a WRN exonuclease-dead mutant (19). POT1 stimulation of human RecQ helicases WRN and BLM does not extend to bacterial helicase RecQ.

POT1 does not enhance the retention of WRN on the telomeric substrates during unwinding

POT1's ability to bind WRN (19) may partly explain the species specificity of the stimulation, and suggests that POT1 could potentially retain WRN on the substrate during unwinding. This would increase the helicase processivity by preventing WRN dissociation prior to complete duplex displacement (Figure 1D). To test this more directly, we used an assay that showed the N-terminal domain of minichromosome maintenance (MCM) helicase enhances its ability to remain template committed, thereby acting as a processivity clamp (42). In reactions containing a mix of long and short duplexes, the MCM N-terminus increased the relative ratio of unwound long versus short duplexes (42). Similarly, if POT1 enhances WRN retention on the longer telomeric duplex fork during unwinding, then less protein is available to unwind a short competitor nontelomeric fork. Reactions contained equal molar amounts of TAMRA labeled Tel ds-34 fork (green) and a Cy5 labeled short competitor 22-bp nontelomeric fork (Mix ds-22) (red) and were visualized by fluoroimagery (Figure 7) and in separate channels for quantitation (Figure S6, Supplementary data). To simplify product analysis, exonuclease activity was inhibited on the short

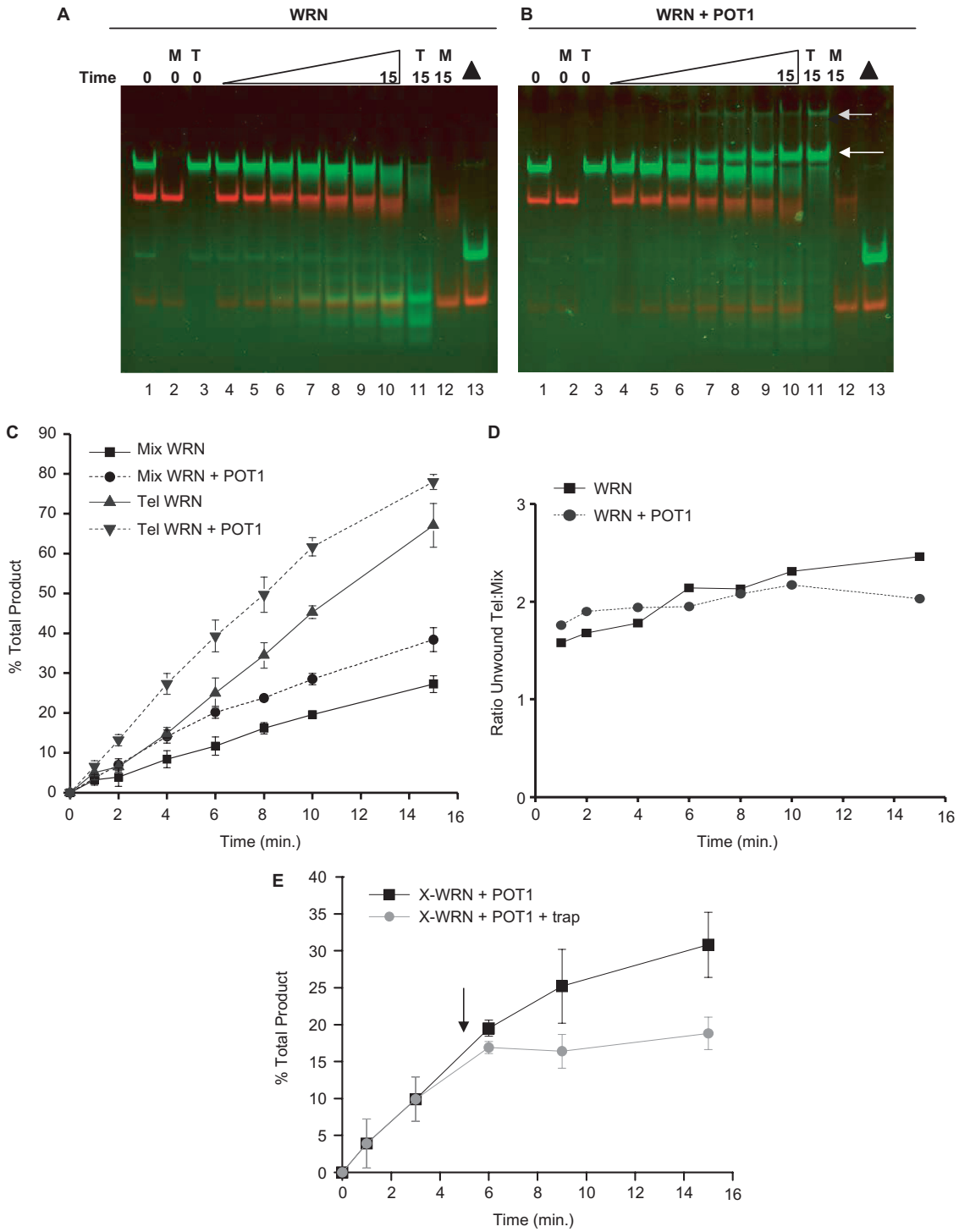

Figure 7. POT1 fails to retain WRN on telomeric substrates during unwinding. The telomeric TAMARA Tel ds-34 fork (green) and nontelomeric Cy5 Mix ds-22 fork (red) were visualized by fluoroimagery with a Typhoon Imager after electrophoresis in 12% native gels. (**A**–**D**) WRN displacement of telomeric versus nontelomeric forks. Reactions contained 1 nM of Tel ds-34 fork (Tl, lanes 3 and 11) or Mix ds-22 fork (Mx, lanes 2 and 12) or both (2 nM total substrate) in standard reaction buffer. Reactions were initiated by adding 10 nM WRN alone (A), or with 80 nM POT1 (B), and aliquots were terminated at 0, 1, 2, 4, 6, 8, 10 or 15 min. Filled triangle, heat denatured substrate; arrow indicates POT1-bound displaced strands. (C) The percent of total displaced product was plotted against time. Mix ds-22 and WRN, filled square and solid black line; Mix ds-22 and WRN + POT1, filled circle and black dotted line; Tel ds-34 and WRN, filled triangle and solid gray line; Tel ds-34 and WRN + POT1, inverted filled triangle and dotted gray line. Values represent the mean and error bars represent the SD from three independent experiments. (D) The ratio of the average of total unwound Tel ds-34 fork versus Mix ds-22 fork was plotted against time. WRN, filled square and solid black line; WRN + POT1, filled circle and gray dotted line. (**E**) Reactions containing 1 nM of TAMRA Tel ds-34 fork and 120 nM POT1 were initiated by adding 30 nM X-WRN and terminated at 0, 1, 3, 6, 9 or 15 min. A nontelomeric Mix ds-34 bp fork (10 nM) was added as a trap at 5 min (arrow) (filled circle and gray line) or omitted (filled square and black line). Total displaced product was plotted against time. Values represent the mean and error bars represent SD from at least two independent reactions.

fork with a thio-linkage at the blunt end. WRN alone displaced shortened strands from the Tel ds-34 fork due to the combined action of the helicase and exonuclease at a rate of 4.4% strand displacement/min, and displaced less Mix ds-22 fork (1.9% strand displacement/min) since the exonuclease could not contribute (Figure 7A and C). POT1 addition to the WRN reactions generated TAMRA bands migrating above the Tel ds-34 substrate that increased as a function of time (Figure 7B). These bands are attributed to full length POT1 (gray arrow) and POT1 fragments (white arrow) bound to the telomeric ssDNA products from the WRN helicase reaction, and are included as product in the calculation for total strand displacement for several reasons. First, proteolysis of POT1 after addition of stop dye is inefficient because SDS detergent was omitted due to interference with the fluoroimeragy. SDS also normally displaces any incompletely digested POT1 protein from the ssDNA product. Second, these upper bands appear after POT1 addition to previously boiled Tel ds-34 forks (lanes 6–8 and 10–12), but not to intact forks (lanes 2–4) (Figure S4, Supplementary data). Finally, the bands migrating above the substrate are not apparent after removal of the proteins from the terminated reactions by chloroform extraction (Figure S5, Supplementary data), although the product bands are less defined and amenable to quantitation. POT1 increased the amount of total displaced Tel ds-34 and Mix ds-22 products at each time point, and slightly increased the overall rate of strand displacement to 6.3 and 2.8% strand displacement/min for both Tel ds-34 and Mix ds-22, respectively (Figure 6C and D). As a result, POT1 addition did not significantly alter the ratio of unwound Tel ds-34 versus Mix ds-22 as a function of time (Figure 6D) or POT1 concentration (data not shown). These data suggest that POT1 does not enhance the retention of WRN on the telomeric substrate during unwinding.

To further test the effect of POT1 on WRN helicase processivity, we examined WRN unwinding of the Tel ds-34 fork in the presence of POT1 after addition of a trap which prevents further initiation events. A similar assay was used to test the effect of MutL on UvrD helicase processivity (43). To more directly examine WRN helicase activity, we used an exonuclease-dead WRN mutant that is also stimulated by POT1 (19) (Figure S7, Supplementary data). The trap consisted of a 10-fold excess of unlabeled nontelomeric 34-bp fork that is not fully unwound by WRN helicase and does not bind POT1 (19). Adding the trap after 5 min quenched the reaction and prevented further strand displacement (Figure 7E). If POT1 acted as a processivity clamp, the amount of unwound telomeric forks should have continued to increase after trap addition, indicating that WRN molecules already engaged on the telomeric forks were able to complete unwinding before dissociating from the substrate. Since no increase was observed (Figure 7E), this shows that WRN protein dissociated even in the presence of POT1 and was effectively trapped by the excess of competitor substrate.

DISCUSSION

Previous studies showed POT1 stimulates WRN and BLM RecQ helicases to unwind longer telomeric duplexes that are poorly unwound by these helicases alone (19). POT1 alters the pattern of WRN helicase/exonuclease products to favor displacement of longer strands by increasing the helicase apparent processivity, rather than by inhibiting the WRN exonuclease directly. Consistent with this, we showed that POT1 alters the WRN product distribution even when the POT1-binding sequences are not on the strand being digested (Figure 5), and that POT1 does not alter WRN digestion of telomeric forks in the absence of helicase activity (Figure S3, Supplementary data). In the current study, we set out to determine the mechanism of helicase stimulation by testing two nonmutually exclusive possibilities (i) POT1 recruitment and retention of WRN on the telomeric substrate to increase unwinding processivity, and/or (ii) POT1 binding to partially unwound strands to prevent their re-annealing upon WRN dissociation (Figure 1).

The first model of a processivity clamp is not supported by the data for several reasons. Although there is evidence that POT1 interacts with WRN (19), POT1 did not recruit WRN to the telomeric substrates tested here. POT1 preloading was not sufficient to stimulate WRN helicase (Figures 2 and 3) or enhance WRN binding (Figure 4). Instead, we favor the second model, whereby POT1 increases WRN helicase apparent processivity by loading on the partially unwound strand to prevent re-annealing. First, POT1 stimulated WRN unwinding only on substrates with POT1-binding sites in the duplex region to be unwound (Figure 2) (19). The finding that POT1 preloading on the 3′-tail of a telomeric duplex fork enhanced stimulation of WRN helicase (Figure 5) could be consistent with a recruitment mechanism. However, POT1 loading at the fork junction was primarily responsible for the enhanced WRN stimulation. We propose POT1 may promote melting of the duplex by binding to the ssDNA at the fork junction, similar to RPA, which can passively melt short duplexes by binding to ssDNA (44). Second, POT1 failed to retain WRN on the telomeric substrate during unwinding in two independent assays (Figure 7). If POT1 retained/clamped WRN on the long telomeric fork during unwinding, this would have sequestered WRN away from the competitor short nontelomeric fork (Figure 7A–D). However, POT1 increased the amount of each fork unwound at all time points, and thus, slightly increased the rate of total strand displacement for both forks (Figure 7C). This agrees with the previous finding that POT1 increases the strand displacement rate of the 34-bp telomeric fork by WRN helicase (19). POT1 binding to the partially unwound strand allows the helicase to continue unwinding from the point of WRN dissociation, leading to more rapid displacement of the remaining duplex, thereby increasing the availability of WRN for both forks. This assay further demonstrated that POT1 is loading on the WRN displaced strands, as indicated by a shift in the telomeric product bands in the presence of POT1 (Figure 7).

Consistent with the hypothesis that POT1 stimulates WRN helicase by preventing strand re-annealing rather than WRN dissociation, is evidence that a WRN and POT1 physical interaction is not essential for helicase stimulation, at least for the substrates tested. The POT1 C-terminal domain is required for precipitating WRN protein from HeLa nuclear extracts, but not for stimulating WRN helicase *in vitro* (19). Since the WRN domain that interacts with RPA is necessary for optimal unwinding of longer duplexes (>50 bp) (27), it is possible that the physical interaction between POT1 and WRN is more important for unwinding duplexes longer than 36 bp. Nevertheless, our data indicate that a cooperative or productive spatial loading of the WRN and POT1 onto DNA molecules is likely critical for the stimulation. The heterologous single-stranded binding (SSB) proteins from *E. coli* and T4 phage and human Rad 51 could not stimulate WRN helicase (19,45). Our current finding that human POT1 does not stimulate *E. coli* RecQ helicase strengthens the importance of species specificity for the WRN and POT1 interaction. Similarly, *E. coli* RecQ is also not stimulated by human RPA or T4 phage SSB protein, but is stimulated by *E. coli* SSB (46). The reason for the species specificity maybe related in part to physical interactions, but also to protein loading in a cooperative and productive manner. POT1 stimulates WRN unwinding of telomeric duplex forks whether the POT1-binding sites are on the same strand the helicase translocates on (Figure 5) or the opposite strand (Figure 2). These proteins appear to be optimally positioned on forked substrates to allow for POT1 loading as WRN reveals POT1-binding sites, and reciprocally POT1 coated 3′-tails do not impede WRN loading and unwinding of forked duplexes (Figures 2 and 5). However, this cooperation is substrate dependent as POT1 preloading blocks WRN unwinding of 3′-tailed telomeric duplexes (Figure 3). Thus, POT1 interactions with the substrate and the ssDNA/dsDNA junction are likely more critical determinants of WRN helicase stimulation, rather than POT1 interactions with the helicase itself.

Genetic studies in fission yeast support a role for POT1 in regulating RecQ helicase activity at telomeric ends. Kibe *et al*. (47) found that a strain expressing a mutant RPA exhibits defects in telomere maintenance and DNA repair, but not in DNA replication. Loss of telomeric protein Taz1 in this mutant RPA strain causes rapid telomere loss, which is suppressed by either overexpressing POT1 or by inactivating RecQ helicase Rqh1 (47). Loss of Taz1 induces replication fork stalling at telomeres (48), which could recruit Rqh1 and higher amounts of mutant RPA at the telomeres may compete with POT1 and stimulate inappropriate helicase activity (47). Kibe *et al*. (47) suggest that POT1 binding to the ssDNA/dsDNA junction at telomeric tails prevents helicase unwinding and fraying of the end. Our biochemical data support this model and show that POT1 inhibited WRN activity on 3′ telomeric tailed duplexes, whereas RPA stimulated WRN activity (Figure 3). POT1 determines the terminal sequence of the recessed 5′-end of telomeres on the C-rich strand which is consistent with POT1 binding to the ssDNA/dsDNA junction at telomeres to regulate processing (39). Furthermore, studies in mice show POT1 loss induces telomerase-independent extension of the G-rich strand presumably through resection of the complementary C-rich strand (26,49). In S-phase, the telomeres exist in an open accessible form that could be susceptible to fraying (50). Therefore, whether telomeric tails are coated with RPA or POT1 could have profound effects on telomere processing.

POT1 and WRN are both implicated in the dissociation of alternate structures at telomeres to suppress aberrant recombination and facilitate replication. Defects in WRN helicase or POT1 homologs in mammalian cells leads to elevated telomeric sister chromatid exchanges, telomere circles, and preferential loss of telomeres replicated from the G-rich lagging strand (24,25,51). Telomere circles are proposed to result from aberrant recombination (7), and both WRN helicase and exonuclease activities are required to suppress their formation (51). This suggests that both activities contribute to the processing of recombination intermediates, consistent with previous reports (52). Our data support the model that POT1 cooperates with WRN to dissociate inappropriate telomeric recombination intermediates, as well as G-quadruplex structures that can form during telomere lagging strand replication. Forks are inherent structures in recombination-type D-loops, which are also substrates for WRN helicase and exonuclease and POT1 simulation of WRN (19,20). Thus, our findings with the forks are also relevant to D-loops. POT1 loading on the ssDNA molecules during WRN unwinding (Figure 7), and POT1 regulation of WRN exonuclease (Figures 2, 3, 5 and 7), are consistent with POT1 roles in protecting the telomeric 3′-tail from excessive degradation as it is released. Furthermore, POT1 stimulates WRN helicase even when binding the same strand that the helicase translocates along (Figure 5), which would be required for the cooperative dissociation of G-quadruplexes at telomeres during lagging strand replication. In summary, we show that while POT1 does not enhance WRN retention on telomeric substrates, POT1 interaction with ssDNA/dsDNA junctions of the substrates regulates WRN protein activity. Defining the substrates on which WRN cooperates with telomeric proteins *in vitro*, should increase our understanding of WRN's role in telomere preservation.

ACKNOWLEDGEMENTS

We thank Dr Vilhelm Bohr (NIA) for the baculoviral stocks for production of WRN and X-WRN proteins. We also thank Dr Walter Chazin and Dalyir Prettor for RPA protein, the production of which was supported by NIH grant GM65484 (W.J.C.), and Dr James Keck for generously providing purified *E. coli* RecQ helicase. We also thank the Opresko lab for critical reading of the article. This work was funded by NIH grant ES0515052 (P.L.O.) and the Ellison Medical Foundation (P.L.O.). Funding to pay the Open Access publication charges for this article was provided by NIH grant ES0515052 (P.L.O.).

Conflict of interest statement. None declared.

REFERENCES

1. Kudlow,B.A., Kennedy,B.K. and Monnat,R.J. Jr. (2007) Werner and Hutchinson-Gilford progeria syndromes: mechanistic basis of human progeroid diseases. *Nat. Rev. Mol. Cell Biol.*, **8**, 394–404.
2. Yu,C.E., Oshima,J., Fu,Y.H., Wijsman,E.M., Hisama,F., Alisch,R., Matthews,S., Nakura,J., Miki,T., Ouais,S. *et al.* (1996) Positional cloning of the Werner's syndrome gene. *Science*, **272**, 258–262.
3. Brosh,R.M. Jr and Bohr,V.A. (2007) Human premature aging, DNA repair and RecQ helicases. *Nucleic Acids Res.*, **35**, 7527–44.
4. Huang,S., Li,B., Gray,M.D., Oshima,J., Mian,I.S. and Campisi,J. (1998) The premature ageing syndrome protein, WRN, is a $3' \rightarrow 5'$ exonuclease. *Nat. Genet.*, **20**, 114–116.
5. Wu,L. and Hickson,I.D. (2006) DNA helicases required for homologous recombination and repair of damaged replication forks. *Annu. Rev. Genet.*, **40**, 279–306.
6. Opresko,P.L. (2008) Telomere ResQue and preservation-roles for the Werner syndrome protein and other RecQ helicases. *Mech. Ageing Dev.*, **129**, 79–90.
7. de Lange,T. (2005) Shelterin: the protein complex that shapes and safeguards human telomeres. *Genes Dev.*, **19**, 2100–2110.
8. Chang,S., Multani,A.S., Cabrera,N.G., Naylor,M.L., Laud,P., Lombard,D., Pathak,S., Guarente,L. and DePinho,R.A. (2004) Essential role of limiting telomeres in the pathogenesis of Werner syndrome. *Nat. Genet.*, **36**, 877–882.
9. Du,X., Shen,J., Kugan,N., Furth,E.E., Lombard,D.B., Cheung,C., Pak,S., Luo,G., Pignolo,R.J., DePinho,R.A. *et al.* (2004) Telomere shortening exposes functions for the mouse Werner and Bloom syndrome genes. *Mol. Cell Biol.*, **24**, 8437–8446.
10. Wyllie,F.S., Jones,C.J., Skinner,J.W., Haughton,M.F., Wallis,C., Wynford-Thomas,D., Faragher,R.G. and Kipling,D. (2000) Telomerase prevents the accelerated cell ageing of Werner syndrome fibroblasts. *Nat. Genet.*, **24**, 16–17.
11. Crabbe,L., Verdun,R.E., Haggblom,C.I. and Karlseder,J. (2004) Defective telomere lagging strand synthesis in cells lacking WRN helicase activity. *Science*, **306**, 1951–1953.
12. Crabbe,L., Jauch,A., Naeger,C.M., Holtgreve-Grez,H. and Karlseder,J. (2007) Telomere dysfunction as a cause of genomic instability in Werner syndrome. *Proc. Natl Acad. Sci. USA*, **104**, 2205–2210.
13. Griffith,J.D., Comeau,L., Rosenfield,S., Stansel,R.M., Bianchi,A., Moss,H. and De Lange,T. (1999) Mammalian telomeres end in a large duplex loop. *Cell*, **97**, 503–514.
14. Bianchi,A., Stansel,R.M., Fairall,L., Griffith,J.D., Rhodes,D. and De Lange,T. (1999) TRF1 binds a bipartite telomeric site with extreme spatial flexibility. *EMBO J.*, **18**, 5735–5744.
15. van Steensel,B., Smogorzewska,A. and De Lange,T. (1998) TRF2 protects human telomeres from end-to-end fusions. *Cell*, **92**, 401–413.
16. Lei,M., Podell,E.R. and Cech,T.R. (2004) Structure of human POT1 bound to telomeric single-stranded DNA provides a model for chromosome end-protection. *Nat. Struct. Mol. Biol.*, **11**, 1223–1229.
17. Opresko,P.L., von Kobbe,C., Laine,J.P., Harrigan,J., Hickson,I.D. and Bohr,V.A. (2002) Telomere-binding protein TRF2 binds to and stimulates the Werner and Bloom syndrome helicases. *J. Biol. Chem.*, **277**, 41110–41119.
18. Machwe,A., Xiao,L. and Orren,D.K. (2004) TRF2 recruits the Werner syndrome (WRN) exonuclease for processing of telomeric DNA. *Oncogene*, **23**, 149–156.
19. Opresko,P.L., Mason,P.A., Podell,E.R., Lei,M., Hickson,I.D., Cech,T.R. and Bohr,V.A. (2005) POT1 stimulates RecQ helicases WRN and BLM to unwind telomeric DNA substrates. *J. Biol. Chem.*, **280**, 32069–32080.
20. Opresko,P.L., Otterlei,M., Graakjaer,J., Bruheim,P., Dawut,L., Kolvraa,S., May,A., Seidman,M.M. and Bohr,V.A. (2004) The Werner syndrome helicase and exonuclease cooperate to resolve telomeric D loops in a manner regulated by TRF1 and TRF2. *Mol. Cell*, **14**, 763–774.
21. Maizels,N. (2006) Dynamic roles for G4 DNA in the biology of eukaryotic cells. *Nat. Struct. Mol. Biol.*, **13**, 1055–1059.
22. Mohaghegh,P., Karow,J.K., Brosh,J.R. Jr, Bohr,V.A. and Hickson,I.D. (2001) The Bloom's and Werner's syndrome proteins are DNA structure-specific helicases. *Nucleic Acids Res.*, **29**, 2843–2849.
23. Orren,D.K., Theodore,S. and Machwe,A. (2002) The Werner syndrome helicase/exonuclease (WRN) disrupts and degrades D-loops in vitro. *Biochemistry*, **41**, 13483–13488.
24. Laud,P.R., Multani,A.S., Bailey,S.M., Wu,L., Ma,J., Kingsley,C., Lebel,M., Pathak,S., DePinho,R.A. and Chang,S. (2005) Elevated telomere-telomere recombination in WRN-deficient, telomere dysfunctional cells promotes escape from senescence and engagement of the ALT pathway. *Genes Dev.*, **19**, 2560–2570.
25. Wu,L., Multani,A.S., He,H., Cosme-Blanco,W., Deng,Y., Deng,J.M., Bachilo,O., Pathak,S., Tahara,H., Bailey,S.M. *et al.* (2006) Pot1 deficiency initiates DNA damage checkpoint activation and aberrant homologous recombination at telomeres. *Cell*, **126**, 49–62.
26. Hockemeyer,D., Daniels,J.P., Takai,H. and de Lange,T. (2006) Recent expansion of the telomeric complex in rodents: two distinct POT1 proteins protect mouse telomeres. *Cell*, **126**, 63–77.
27. Doherty,K.M., Sommers,J.A., Gray,M.D., Lee,J.W., von Kobbe,C., Thoma,N.H., Kureekattil,R.P., Kenny,M.K. and Brosh,R.M. Jr. (2005) Physical and functional mapping of the replication protein a interaction domain of the Werner and bloom syndrome helicases. *J. Biol. Chem.*, **280**, 29494–29505.
28. Opresko,P.L., Laine,J.P., Brosh,R.M. Jr, Seidman,M.M. and Bohr,V.A. (2001) Coordinate action of the helicase and $3'$ to $5'$ exonuclease of werner syndrome protein. *J. Biol. Chem.*, **276**, 44677–44687.
29. Opresko,P.L., Calvo,J.P. and von Kobbe,C. (2007) Role for the Werner syndrome protein in the promotion of tumor cell growth. *Mech. Ageing Dev.*, **280**, 29494–29505.
30. Machwe,A., Xiao,L., Theodore,S. and Orren,D.K. (2002) DNase I footprinting and enhanced exonuclease function of the bipartite Werner syndrome protein (WRN) bound to partially melted duplex DNA. *J. Biol. Chem.*, **277**, 4492–4504.
31. Shen,J.C. and Loeb,L.A. (2000) Werner syndrome exonuclease catalyzes structure-dependent degradation of DNA. *Nucleic Acids Res.*, **28**, 3260–3268.
32. Huang,S., Beresten,S., Li,B., Oshima,J., Ellis,N.A. and Campisi,J. (2000) Characterization of the human and mouse WRN $3' \rightarrow 5'$ exonuclease. *Nucleic Acids Res.*, **28**, 2396–2405.
33. Kamath-Loeb,A.S., Shen,J.C., Loeb,L.A. and Fry,M. (1998) Werner syndrome protein. II. characterization of the integral $3' \rightarrow 5'$ dna exonuclease. *J. Biol. Chem.*, **273**, 34145–34150.
34. Li,B. and Comai,L. (2001) Requirements for the nucleoytic processing of DNA ends by the werner syndrome protein:Ku70/80 complex. *J. Biol. Chem.*, **276**, 9896–9902.
35. Choudhary,S., Sommers,J.A. and Brosh,R.M. Jr. (2004) Biochemical and kinetic characterization of the DNA helicase and exonuclease activities of werner syndrome protein. *J. Biol. Chem.*, **279**, 34603–34613.
36. Machwe,A., Xiao,L. and Orren,D.K. (2006) Length-dependent degradation of single-stranded $3'$ ends by the Werner syndrome protein (WRN): implications for spatial orientation and coordinated $3'$ to $5'$ movement of its ATPase/helicase and exonuclease domains. *BMC Mol. Biol.*, **7**, 6.
37. Verdun,R.E., Crabbe,L., Haggblom,C. and Karlseder,J. (2005) Functional human telomeres are recognized as DNA damage in g2 of the cell cycle. *Mol. Cell*, **20**, 551–561.
38. Brosh,R.M. Jr, Waheed,J. and Sommers,J.A. (2002) Biochemical characterization of the DNA substrate specificity of werner syndrome helicase. *J. Biol. Chem.*, **277**, 23236–23245.
39. Hockemeyer,D., Sfeir,A.J., Shay,J.W., Wright,W.E. and de Lange,T. (2005) POT1 protects telomeres from a transient DNA damage response and determines how human chromosomes end. *EMBO J.*, **24**, 2667–2678.
40. Sharma,S., Otterlei,M., Sommers,J.A., Driscoll,H.C., Dianov,G.L., Kao,H.I., Bambara,R.A. and Brosh,R.M. Jr. (2004) WRN helicase and FEN-1 form a complex upon replication arrest and together process branch migrating DNA structures associated with the replication fork. *Mol. Biol. Cell*, **15**, 734–750.

41. Lei,M., Zaug,A.J., Podell,E.R. and Cech,T.R. (2005) Switching human telomerase on and off with hPOT1 protein in vitro. *J. Biol. Chem.*, **280**, 20449–20456.
42. Barry,E.R., McGeoch,A.T., Kelman,Z. and Bell,S.D. (2007) Archaeal MCM has separable processivity, substrate choice and helicase domains. *Nucleic Acids Res.*, **35**, 988–998.
43. Mechanic,L.E., Frankel,B.A. and Matson,S.W. (2000) Escherichia coli MutL loads DNA helicase II onto DNA. *J. Biol. Chem.*, **275**, 38337–38346.
44. Lao,Y., Lee,C.G. and Wold,M.S. (1999) Replication protein A interactions with DNA. 2. Characterization of double-stranded DNA-binding/helix-destabilization activities and the role of the zinc-finger domain in DNA interactions. *Biochemistry*, **38**, 3974–3984.
45. Brosh,R.M. Jr, Orren,D.K., Nehlin,J.O., Ravn,P.H., Kenny,M.K., Machwe,A. and Bohr,V.A. (1999) Functional and physical interaction between WRN helicase and human replication protein A. *J. Biol. Chem.*, **274**, 18341–18350.
46. Shereda,R.D., Bernstein,D.A. and Keck,J.L. (2007) A central role for SSB in Escherichia coli RecQ DNA helicase function. *J. Biol. Chem.*, **282**, 19247–19258.
47. Kibe,T., Ono,Y., Sato,K. and Ueno,M. (2007) Fission yeast Taz1 and RPA are synergistically required to prevent rapid telomere loss. *Mol. Biol. Cell*, **18**, 2378–2387.
48. Miller,K.M., Rog,O. and Cooper,J.P. (2006) Semi-conservative DNA replication through telomeres requires Taz1. *Nature*, **440**, 824–828.
49. He,H., Multani,A.S., Cosme-Blanco,W., Tahara,H., Ma,J., Pathak,S., Deng,Y. and Chang,S. (2006) POT1b protects telomeres from end-to-end chromosomal fusions and aberrant homologous recombination. *EMBO J.*, **25**, 5180–5190.
50. Verdun,R.E. and Karlseder,J. (2006) The DNA damage machinery and homologous recombination pathway act consecutively to protect human telomeres. *Cell*, **127**, 709–720.
51. Li,B., Jog,S.P., Reddy,S. and Comai,L. (2008) WRN controls formation of extrachromosomal telomeric circles and is required for TRF2DeltaB-mediated telomere shortening. *Mol. Cell Biol.*, **28**, 1892–1904.
52. Swanson,C., Saintigny,Y., Emond,M.J. and Monnat,R.J. Jr. (2004) The Werner syndrome protein has separable recombination and survival functions. *DNA Repair*, **3**, 475–482.